Mechanics of Materials 43 (2011) 25–35

Contents lists available at ScienceDirect

Mechanics of Materials

journal homepage: www.elsevier.com/locate/mechmat

A novel and general form of effective stress in a partially saturated porous material: The influence of microstructure

Ivan Vlahinić [a,*], Hamlin M. Jennings [b], José E. Andrade [c], Jeffrey J. Thomas [d]

[a] Northwestern University, Evanston, IL 60208, USA
[b] Massachusetts Institute of Technology, Cambridge, MA 02139, USA
[c] California Institute of Technology, Pasadena, CA 91125, USA
[d] Schlumberger-Doll Research, Cambridge, MA 02139, USA

ARTICLE INFO

Article history:
Received 28 September 2009
Received in revised form 19 September 2010

Keywords:
Effective stress
Partially saturated/unsaturated material
Porous material
Micro-mechanics

ABSTRACT

A recently published constitutive model for drying of a partially saturated porous material is extended to take into account finite air (gas) pressure as well as finite external load, variables that are absent during simple drying under atmospheric conditions. We further use the result to derive a general form of effective stress in a partially saturated material. The proposed framework overcomes a primary shortcoming of the classic Bishop effective stress expression and offers a novel way to incorporate important morphological features. In addition, we show how existing micromechanical homogenization techniques aided by basic descriptions of material morphology may be used to inform the study of elastic deformations in the partially saturated media. We further show that for two very specific schemes, and thus for two particular morphologies of porous materials, the proposed effective stress framework remarkably reduces to a volumetric *average pressure* form which is commonly encountered in literature. In this work, we also provide an extensive discussion and critique of the classic Bishop effective stress approach.

1. Introduction to effective stress

1.1. Fully saturated effective stress

The concept of 'effective stress' is extremely useful in the analysis of fluid-saturated porous materials and is cited as perhaps the single most fundamental contribution to the study of such materials (e.g. Khalili et al., 2004). It extends the classic theories of deformable solids to deformable porous fluid-filled solids. Under a single term, the effective stress additively combines disparate contributions of fluid pressure(s) and externally applied load(s), and allows a fluid-filled material to be analyzed as if it were dry, a striking simplification. This has enabled the development of a great number of constitutive models for porous materials (e.g. Schofield and Wroth, 1968; Grueschow and Rudnicki, 2005).

Paul Fillunger and Karl von Terzaghi discovered fundamental mechanical effects in a porous solid saturated by a single fluid in the first half of the 20th century (de Boer, 1992), which led them to the concept of 'effective stress'. But it was not until the second half of the century that Geertsma (1957) and Skempton (1961) independently defined the general effective stress expression in a fully saturated material, one which also accounts for the relative deformability of the solid structure. Their expression was later mathematically derived by Nur and Byerlee (1971). These contributions facilitated a wider appeal, extending the applicability of the concept beyond the so-called 'rigid' or 'incompressible' porous materials and provided a more solid theoretical footing to Terzaghi's and Fillunger's phenomenological expression.

* Corresponding author. Tel.: +1 8474917161; fax: +1 8474914011.
E-mail addresses: ivan@u.northwestern.edu (I. Vlahinić), hmj@mit.edu (H.M. Jennings), jandrade@caltech.edu (J.E. Andrade), JThomas39@slb.com (J.J. Thomas).

0167-6636/$ - see front matter © 2010 Elsevier Ltd. All rights reserved.
doi:10.1016/j.mechmat.2010.09.007

For a porous material saturated with a single fluid, the effective stress is:

$$\boldsymbol{\sigma}^{eff} = \boldsymbol{\sigma} - \zeta p\ \boldsymbol{\delta} \tag{1}$$

where

$$\zeta = 1 - K_b/K_s \quad \text{(Biot coefficient)}$$

where bold letters indicate a tensorial quantity and where $\boldsymbol{\sigma}^{eff}$ is the effective stress, $\boldsymbol{\sigma}$ is the total external stress, p is the pore pressure, $\boldsymbol{\delta}$ is the Kronecker delta, K_b is the drained bulk modulus (of the porous solid), and K_s is the bulk modulus of the solid or grain.

It should be noted that inherent material microstructural features of the porous material play an important role in Eq. (1), although at glance this is not readily apparent. For example, the volume of porosity factors into the effective stress via the Biot coefficient ζ, or rather via the ratio of the material properties K_b/K_s; all else being equal, the ratio tends to decrease as the porosity of the dry system increases. Also the geometry of the porous space plays an integral role. For example, materials whose pore spaces are a collection of narrow openings, which is often the case in materials measuring high pore surface area but low pore volume, tend to suffer from low drained bulk stiffness, making $\zeta \simeq 1$. An excellent example of this is provided by the studies of Westerley granite, a rock known to contain a network of fractured surfaces (Nur and Byerlee, 1971, p. 6418, Fig. 3). Despite the fact that pores occupy merely one percent of the granite's total volume, K_b is an order of magnitude lower than K_s.[1] Various sands and clays also tend to fall in this category. In general, materials in which $K_s \gg K_b$, and consequently $\zeta \simeq 1$, are often referred to as 'incompressible'; for these materials, the effective stress expression simplifies to Terzaghi's original postulate, namely that $\boldsymbol{\sigma}^{eff} = \boldsymbol{\sigma} - p\boldsymbol{\delta}$.

On the other hand, a material with pore spaces of relatively symmetrical dimensions tends *not* to have a degraded drained modulus. Consequently, the ratio of K_b/K_s in such material is typically finite and not negligible. For example, the ratio K_b/K_s in cement paste with 28% capillary porosity is approximately 1/6 while in Vycor^{tm} glass of similar porosity, the ratio is slightly less than 1/3 (Vlahinić et al., 2009). In sintered glass of similar porosity the ratio is slightly higher than 1/2 while for the same material with 5% porosity, the ratio is 9/10 (Walsh et al., 1965, p. 607, Fig. 2). The error in assuming solid incompressibility in order to quantify the effective stress for these materials is apparent. Nur and Byerlee (1971, Fig. 2) provide excellent experimental evidence of errors involved in measuring volumetric strains via jacketed and unjacketed pore pressure tests on Weber sandstone with 6% porosity. These examples all indicate the importance of microstructural features, via parameter ζ, to accurately predict or interpret from experiments the strains for a very diverse group of materials.

[1] Based on the experimental evidence provided, this appears true for confining pressures less than 100 MPa. At greater pressures, the cracks close due to high confinement and the material behaves as if it were pore- or crack-free.

1.2. Partially saturated effective stress

In the case of partially saturated materials, several researchers appear to have independently published very similar expressions defining the effective stress in the years prior to a 1960 conference held in London on the pore pressure and suction of soils (Jennings and Burland, 1962). In the end it was the most general expression which included the term for the pressure in the gas phase that won the day, originally proposed by Bishop (1955) and submitted to the conference by Aitchison and Bishop (1960). The authors argued that in the presence of multiple fluids the contribution of each fluid to the overall effective stress should be averaged according to the fractional contact area between the individual fluids and the representative unit area of the material[2], termed the Bishop parameter χ. In this work we use water and air as model fluids leading to $p = \chi p_w + (1-\chi)p_a$, although the formulation applies to any other fluid combination as well, e.g. oil and water. On this basis, the classic effective stress expression for a partially saturated material reduces to:

$$\boldsymbol{\sigma}^{eff} = \boldsymbol{\sigma}^{net} + \chi\zeta p_{cap}\boldsymbol{\delta} \quad \text{(classic eff. stress)} \tag{2}$$

where

$$\boldsymbol{\sigma}^{net} = \boldsymbol{\sigma} - \zeta p_a \boldsymbol{\delta} \quad \text{(net stress)}$$
$$\zeta = 1 - K_b/K_s \quad \text{(Biot coefficient)}$$
$$p_{cap} = p_a - p_w \quad \text{(capillary stress)}$$

where $\boldsymbol{\sigma}^{net}$ is the net stress, p_a is the air pressure, p_w is the water pressure, and p_{cap} is the capillary pressure (suction) defined as the difference between the two fluid pressures. Often, a particular solution and a slight simplification involves setting $\zeta = 1$, which physically reflects the assumption of solid incompressibility as discussed earlier.

The primary concern with Eq. (2) rests in quantifying χ, which is expected to be found on an empirical basis as a function of the degree of saturation, varying from zero for a dry porous system to unity for a fully saturated porous system. It should also be noted that the Biot coefficient in Eq. (2) is not found in the original works of Bishop and other researchers. Today however, ζ is generally included in Eq. (2) as in e.g. Lewis and Schrefler (1987) presumably on the grounds that in the extremes, a partially saturated effective stress ought to reduce to a fully saturated effective stress which was long shown to contain this parameter (see Eq. (1)).

Historically, some authors have expressed reservations with the use of Eq. (2) on the grounds that apparently no unique relationship exists between χ and the degree of saturation, S_w. Coleman (1962) rightly pointed out that χ is a parameter related to the material structure and concluded that it should not be surprising if correlation with S_w is not found (Khalili et al., 2004). Khalili and Khabbaz (1998) found that a relationship can be obtained when plotting χ against a parameter that is a function of suction. Others (e.g., Fredlund and Morgenstern, 1977) have argued that a stress variable should be independent of material

[2] For a precise physical meaning of χ, see discussion in Section 3.1 along with Fig. 2.

parameters altogether. We later show that based on our proposed formulation indirect quantification of χ in terms of the degree of saturation is possible.

1.3. General constitutive modeling of partially saturated materials

Despite some progress using the single effective stress variable, many authors have supported the use of an additional variable to model the general mechanical behavior of partially saturated materials. In an excellent review article, Gens et al. (2007) has suggested that a second variable is generally required to represent the (de)stabilizing influence of suction on shear strength and volume change. A review of many models using two independent stress variables can be found in Alonso and Delage (1996).

Early proponents of the 'two stress variable' approach included Bishop and Blight (1963) and Fredlund and Morgenstern (1977), whose models relied on the use of a net stress $\boldsymbol{\sigma}^{net}$ and a capillary pressure p_{cap}, while more advanced models that emanated from this approach can be found in the works of Alonso et al. (1990) and Wheeler and Sivakumar (1995). Recently however, an alternative two variable approach has been advanced to allow the partially saturated models to be more easily incorporated into the existing fully saturated material models. The approach entails replacing the net stress $\boldsymbol{\sigma}^{net}$ with a form of the full Bishop effective stress $\boldsymbol{\sigma}^{eff}$ while keeping the other scalar variable p_{cap} untouched (e.g., Sheng et al., 2004; Santagiuliana and Schrefler, 2006). The main advantage is that the Bishop effective stress naturally reduces to a fully saturated or dry form in the extremes of $S_w = 1$ or $S_w = 0$, respectively, insuring a seamless continuity, whereas the net stress does not. Ironically, due to the greater complexity of the Bishop effective stress over net stress, the former formulation also tends to lead to simpler constitutive models (Sheng et al., 2008).

Whether making use of one or two variables one thing is clear: the Bishop effective stress continues to play a key role in mechanical modeling of partially saturated materials. Yet the expression itself is quantifiable only on an empirical basis since the fractional fluid contact area χ is inherently an empirical parameter. Other limitations of the Bishop effective stress are discussed in Section 3.1.

2. A novel form of effective stress in partially saturated media: homogenized modulus

2.1. Brief review of our previous work

In this section we theoretically derive a new and general form of effective stress in partially saturated media from macroscopic arguments. We extend our recent work (Vlahinić et al., 2009) on drying of the porous media to a material infiltrated by water and air to include finite air pressure as well as finite external load, variables that are generally absent during drying under atmospheric conditions. Previously, we found that a material parameter termed *effective bulk modulus* (and not pressure averaging) is critical for proper predictions of volumetric deformations during drying. By extension, the proposed effective stress expression will be shown to also contain this parameter.

We now briefly review the results of our previous work on a simple drying of a partially saturated porous material. In Fig. 1, we assume that the pores of arbitrary shape are interconnected and homogeneously distributed. We further assume that water occupies a fraction of the total pore volume and imposes a uniform tensile pressure wherever it makes contact with the pore walls of the solid. The tensile pressure is generated by the formation of capillary menisci. The pressure in the gas phase (in this case air) is assumed inconsequential in comparison to the capillary pressure (suction), which is an order of magnitude higher at relative humidities as high as 98%.

Under these boundary conditions, the total volumetric strain at equilibrium of the system in Fig. 1 reduces to:

$$\varepsilon_v = p_{cap}\left(\frac{1}{K_b} - \frac{1}{\overline{K}}\right) \tag{3}$$

where $\overline{K}$ which describes a homogenized modulus of an *effective solid* (consisting of the solid phase and the empty (air) pores) depends on the degree of saturation, S_w. It was further shown that at any given degree of saturation the total volume of air-filled pores divided by the overall volume of the *effective solid*, termed porosity of the *effective solid*, φ, reduces to:

$$\varphi(S_w) = \frac{(1 - S_w)\phi_o}{1 - S_w\phi_o}; \quad 0 \leqslant \varphi(S_w) \leqslant \phi_o \tag{4}$$

where ϕ_o is the overall porosity of the dry system (Vlahinić et al., 2009).

We note that our formulation is not concerned with the detailed microscale mechanisms of deformation. Rather, the overall solution contains macroscopically averaged or homogenized material properties, the drained bulk modulus and the bulk modulus of the *effective solid*.

2.2. The proposed effective stress expression controlling the volume change

To arrive at a more general constitutive behavior of partially saturated media it is necessary to include both an external load and a finite air pressure. For simplicity we deal with the air pressure p_a and the external confining pressure $\bar{\sigma}$ first; the remaining deviatoric external stresses will be included later.

To this end, let us assume that prior to drying, the porous material has already undergone elastic straining and that the pre-strain has resulted from the external confining pressure and the air pressure of any value. Under the assumption of linear elasticity it is sufficient to superimpose the strain field caused by the preload to the strain field which has resulted from a simple drying. Noting that the strains from the preload are identical those of an externally loaded system fully saturated by the air phase, the total volumetric strain reduces to:

$$\varepsilon_v = \underbrace{\frac{\bar{\sigma} - p_a}{K_b} + \frac{p_a}{K_s}}_{\text{pre-strain}} + \underbrace{p_{cap}\left(\frac{1}{K_b} - \frac{1}{\overline{K}}\right)}_{\text{drying strain}} \tag{5}$$

After some reorganizing of Eq. (5), the general effective pressure $p^{eff} = K_b\varepsilon_v$ simplifies to:

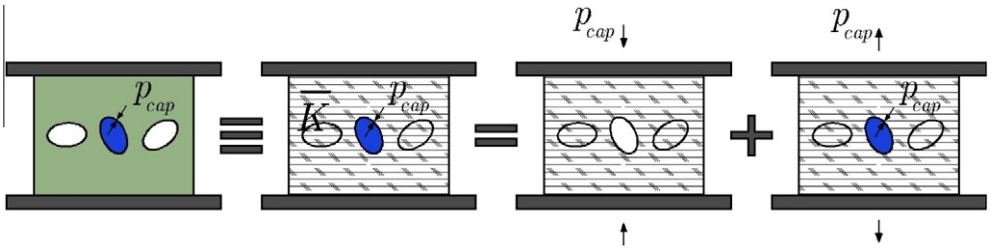

Fig. 1. 1D schematic of stress superposition in a drying unsaturated porous material, where the air pressure is assumed inconsequential and the external loads are omitted for simplicity. The ellipsoidal openings represent a collection of pores rather than individual cavities. Note that the capillary pressure acts over only a portion of the interior solid surface, in contrast with the fully saturated system. Due to these non-uniform boundary conditions, the state of strain in the underlying solid will also be non-uniform even under equal confining and capillary pressures. In the proposed effective stress formulation, this observation is taken into account on a macroscopic basis, via an effective or homogenized material parameter $\overline{K}$.

$$p^{eff} = \left(\bar{\sigma} - p_a\left(1 - \frac{K_b}{K_s}\right)\right) + p_{cap}\left(1 - \frac{K_b}{\overline{K}}\right) \tag{6}$$

Further adding the external deviatoric stresses and noting that under quasi-static conditions the fluid cannot resist shear stresses (i.e. viscous effects in the fluids are negligibly small), we arrive at a complete effective stress in partially saturated media:

$$\boldsymbol{\sigma}^{eff} = \boldsymbol{\sigma}^{net} + \bar{\zeta} p_{cap}\boldsymbol{\delta} \quad \text{(proposed eff. stress)} \tag{7}$$

where

$$\boldsymbol{\sigma}^{net} = \boldsymbol{\sigma} - \zeta p_a \boldsymbol{\delta} \quad \text{(net stress)}$$
$$\zeta = 1 - K_b/K_s \quad \text{(Biot coefficient)}$$
$$\bar{\zeta} = 1 - K_b/\overline{K} \quad \text{(eff. Biot coefficient)}$$
$$p_{cap} = p_a - p_w \quad \text{(capillary stress)}$$

Just as we term $\overline{K}$ an *effective* bulk modulus, we term $\bar{\zeta}$ an *effective* Biot coefficient representing a homogenized property. As a final check, we also note that the general solution in Eq. (7) in fact reduces to the solution for simple drying given by Eq. (3) for the case of no external loads and null air pressure.

Comparing the classic Bishop effective stress in Eq. (2) and the effective expression proposed in Eq. (7) we outline the following key differences:

- The term(s) multiplying the capillary pressure differ in the two expressions.
- A seamless continuity between the fully and partially saturated states is insured in both expressions. But whereas the classic Bishop's effective stress bridges the fully and partially saturated states by averaging the pressure, the proposed effective stress guarantees the continuity via a material parameter $\overline{K}$, or by extension via a parameter we term an effective Biot coefficient $\bar{\zeta}$.
- The classic Bishop effective stress is inherently empirical since the Bishop parameter χ cannot be explicitly related to the degree of saturation S_w. On the other hand, the proposed effective stress expression relies on the effective bulk modulus, $\overline{K}$, which can be quantified using homogenization methods. The methods are discussed in Appendix A and used to evaluate the Bishop parameter, χ, in Section 4.

3. A particular form of the partially saturated effective stress

3.1. The 'intergranular stress' concept in fully and partially saturated media

Terzaghi's and Fillunger's effective stress expression has been useful in many practical, fully saturated soil mechanics problems. But by the middle of the 20th century, tests on various porous rocks and concrete showed limitations and this began to reinforce the idea that a general effective stress expression for fully saturated materials is in fact more complex than originally assumed. The additional complexity at this time was commonly attributed to the intergranular stress acting between the neighboring particles or grains (Bishop and Eldin, 1950; Skempton, 1961). Per schematic at left of Fig. 2, this suggested that the fully saturated effective stress should be:

$$\boldsymbol{\sigma}^{eff} = \boldsymbol{\sigma} - (1 - a_s)p_w\boldsymbol{\delta} \tag{8}$$

where a_s is the contact area of the particles per unit cross-sectional area of the material. When the gross area of particle contacts a_s is sufficiently small, Eq. (8) reduces to Terzaghi's and Fillunger's approximation; otherwise, no simple reduction can be made. However, this line of reasoning has little applicability to porous materials composed of a continuous solid matrix where the meaning of the "particle contact area" is not entirely clear. The reasoning also breaks down even in granular materials. After Laughton (1955) successfully measured the cross-sectional contact areas of hydrostatically compressed lead shot, a granular medium, Skempton (1961) deduced that the errors in estimating the effective stress on the basis of intergranular stress were far in excess of experimental error. More specifically, it was found that even when the average contact area of lead shot approached unity, the effective stress did not deviate significantly from Terzaghi's and Fillunger's original postulate. Instead, Eq. (1) was shown to be correct on experimental and theoretical basis by several researchers (e.g. Skempton, 1961; Nur and Byerlee, 1971) while the references to Eq. (8) are seldom found anywhere in modern literature.

Despite the fact that the intergranular stress does *not* represent the effective stress for a fully saturated porous material as noted above, the intergranular stress concept continues to be used in describing the effective stress in

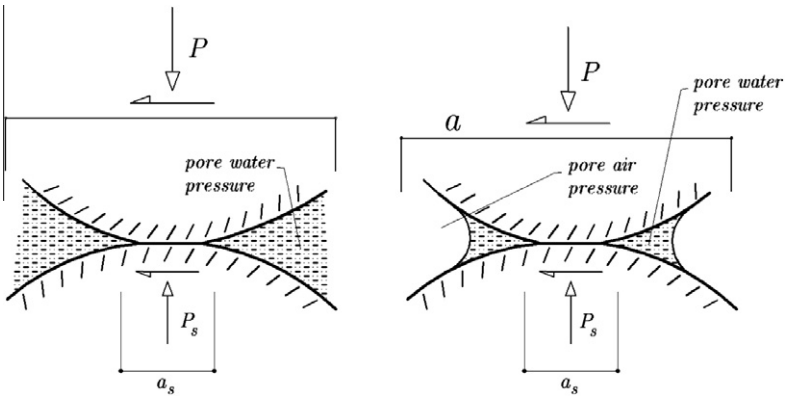

Fig. 2. Intergranular stresses in fully (at left) and partially (at right) saturated material, adopted from Skempton (1961). The effective stress was long thought to be equal to the intergranular stress between the neighboring solid particles or grains. For the fully saturated materials, this approach has long fallen out of favor after Skempton (1961) showed large discrepancies with experiments on lead shot. In partially saturated materials, the approach continues to be used and cited as the Bishop stress after the work of Bishop (1955), Aitchison and Bishop (1960). See text for additional details.

partially saturated materials, whether the materials are composed of individual grains or not. Furthermore it is used exclusively under the assumption that the contact area between the particles or grains is negligible, i.e. $a_s \ll 1$. Per schematic at right of Fig. 2, this means that the partially saturated effective stress reduces to:

$$\boldsymbol{\sigma}^{eff} = \boldsymbol{\sigma} - (\chi p_w + (1-\chi)p_a)\boldsymbol{\delta}, \tag{9}$$

where water pressure p_w acts over an area χ per unit cross-sectional area of the porous material and where air pressure p_a acts over an area $1-\chi$ per unit cross-sectional area. In fact, this simple derivation is how Bishop and other researchers[3] arrived at a form of Eq. (2). Therefore while ubiquitous in literature, it appears that the Bishop effective stress which is based on the concept of intergranular stress, should be used with caution.

3.2. Limitations of a popular simplification, $\chi = S_w$

A common and popular form of Eq. (9) is found by equating the Bishop parameter χ to the degree of saturation S_w:

$$\boldsymbol{\sigma}^{eff} = \boldsymbol{\sigma} - (S_w p_w + (1-S_w)p_a)\boldsymbol{\delta} \tag{10}$$

Hassanizadeh and Gray (1980) deduced the relationship from the entropy inequality for multiphase flow, Lewis and Schrefler (1987) via the macroscopic volume averaging, and Hutter et al. (1999) on the basis of mixture theory. It should be noted that in the aforementioned formulations, the Biot coefficient does not appear in the derivation and is instead added a posteriori as a corrective term, whereas our formulation requires no corrective terms since ζ appears naturally in Eq. (7).

From the perspective of microporomechanics, Dormieux et al. (2006) conclude that only when there is no morphological difference between the water and air filled pore domains, the Bishop stress reduces to the popular form $\chi = S_w$. More recently on the basis of energy arguments, Coussy (2008) has explored the implications of the Bishop's effective stress and has found that Eq. (10) is based on the restrictive assumption of the iso-deformation of the porous networks. In other words, only under the assumption that the porous volumes occupied by the two fluids in a partially saturated material undergo the same straining does one recover the correct state equations of poroelasticity.

The apparent coincidence in the results of various approaches, however, should not be taken to mean that Eq. (10) must be employed in studying partially saturated media. Gray and Schrefler (2001) outline practical applications where Eq. (10) has been successfully employed, e.g. the correct prediction of the failure behavior of earthdams under seismic loads (Zienkiewicz et al., 1999), but also carefully note the limitations. Vlahinić et al. (2009) found the expression inadequate in describing the elastic volumetric drying strains of cement paste and porous glass and Gudehus (1995) concluded that a different expression for χ altogether models well the response of fine-grained soils in triaxial tests.

Collectively, the above observations point out the limitations of Eq. (10). In the next section, we show how the effective stress expression in Eq. (10) may be deduced on the basis of our proposed formulation for specific material morphologies.

4. The Bishop parameter: influence of material microstructure

4.1. Quantifying the bishop parameter χ

Let us reemphasize our original and key point, which is that our proposed formulation allows the Bishop parameter (and by extension the effective stress in partially saturated materials) to be quantified apriori, something that previous works have only been able to determine on an empirical basis.[4] A notable exception, and an alternative

[3] As noted in Section 1.2, only Bishop's expression accounted for the pressure in the gas phase.

[4] We continue to use the Bishop parameter χ as the primary variable because the term is omnipresent in literature. However, we note our reservation with the Bishop effective stress as derived from the intergranular equilibrium in Section 3.1.

approach, can be found in the work of (Chateau and Dormieux, 2002 and Dormieux et al., 2006) who developed the macroscopic constitutive relations of a partially saturated medium by rigorous upscaling of the microscopic poroelasticity. On this basis, the authors found that the degree of saturation and the Bishop parameter can ultimately be related although it appears that quantitative estimates of the Bishop parameter using this recipe have not yet been made.

A direct comparison between the classic expression of effective stress in partially saturated materials in Eq. (2) and the new proposed form in Eq. (7) shows that the sole mathematical difference between the two expressions lies in the term multiplying the capillary pressure p_{cap}. Thus, setting the two expressions equal, we find that on the basis of the proposed formulation, the Bishop parameter reduces to:

$$\chi = \frac{\bar{\zeta}}{\zeta} = \frac{1 - (K_b/K_s)/(\overline{K}(\varphi)/K_s)}{1 - K_b/K_s} \tag{11}$$

The presence of $\overline{K}(\varphi)$ in Eq. (11) indicates that the Bishop parameter χ is not only a function of the material fabric but that its value changes depending on the volumetric proportions of fluids occupying the porous domain.

In our previous work (Vlahinić et al., 2009), we used experimental measurements of the solid and of the (drained) bulk compressibility to linearly approximate the value of $\overline{K}$ for two distinct poroelastic materials, 'predried' hardened cement paste and porous glass. We further used this result to evaluate the magnitude of drying strains in these materials and compare them with experimental data. Although we found that the linear estimate yields accurate values of $\overline{K}$ in some cases, it cannot explicitly account for the morphological features. Such estimate also fails to yield reasonable values for $\overline{K}$ in the case of "incompressible" materials, i.e. when the ratio of $K_b/K_s \ll 1$. To this end, in Section 4.4 we show how established micromechanical homogenization techniques aided by basic descriptions of material microgeometry may be used to overcome these limitations.

4.2. $\chi = S_w$ via the Voigt estimate

Here we evaluate K_b and $\overline{K}$, and by extension χ, based on the Voigt estimate. Analogous to a linear mixture theory, the effective bulk modulus of a material via the Voigt estimate (VO) is a volume average of the bulk moduli of the individual phases. The estimate also represents an absolute upper bound of the effective modulus in a two-phase material. The solution to the estimate is found by assuming that both phases of a two-phase material strain equally and uniformly, in a so-called parallel configuration.

In the context of our proposed formulation, the effective bulk modulus $\overline{K}$ based on the Voigt estimate reduces to:

$$\overline{K}^{vo}(\varphi) = (1 - \varphi)K_s \quad \text{(Voigt estimate)} \tag{12}$$

where φ represents the volume fraction of gas filled pores within the *effective solid* at any given state of partial saturation. If the properties of the solid material or grain are known, the drained bulk modulus on the basis of the Voigt estimate, K_b^{vo}, is:

$$K_b^{vo} = \overline{K}^{vo}(\varphi = \phi_o) = (1 - \phi_o)K_s \tag{13}$$

where ϕ_o is the total (drained) porosity. Further noting from Eq. (4) that $\varphi(S_w) = (1 - S_w)\phi_o/(1 - S_w\phi_o)$, we deduce via Eq. (11) that the Bishop parameter χ takes on a strikingly simple form:

$$\chi^{vo} = \frac{1 - (K_b^{vo}/K_s)(K_s/\overline{K}^{vo})}{1 - K_b^{vo}/K_s} = \frac{1 - (1 - \phi_o)(1 - (1 - S_w)\phi_o/(1 - \phi_o))}{1 - (1 - \phi_o)} = \frac{1 - (1 - S_w\phi_o)}{\phi_o}$$
$$\chi^{vo} = S_w \tag{14}$$

Thus we have shown that under the assumption that the porous material properties can be well modeled via a Voigt estimate, our proposed formulation reduces to the simple form of the classic Bishop stress expression given by Eq. (10). However the conclusion may be more of theoretical rather then practical interest. In reality, we expect the strain field in the solid *not* to be uniform even under e.g. equal confining and capillary pressures because the capillary pressure does not act uniformly over all of the interior solid surfaces.

4.3. χ via homogenization schemes: Mori–Tanaka, self-consistent, and differential

We now estimate the Bishop parameter by calculating K_b and $\overline{K}$ using the well established homogenization techniques. A discussion on the merits, applicability, and methods of solution for such techniques is presented in Appendix A. The micromechanical estimates employed in this work are the self-consistent (SC), the differential (DF), and the Mori–Tanaka (MT). These are the most commonly applied estimates in literature. They have been used to calculate effective or homogenized properties for a diverse group of porous materials, including those that are particulate and those that are of matrix-void type, for those that are cracked and those that are not, as indicated in Fig. 3.

We will show that the Bishop parameter remarkably reduces to S_w for materials whose elastic properties are well-described by the MT scheme (we arrived at the same conclusion using the Voigt estimate in the previous section). In general however, the Bishop parameter will not reduce to S_w and will instead take on a value that depends on the assumed/observed morphological features of a given porous material.

In Fig. 5 we show the values of the Bishop parameter based on the results of various schemes in Fig. 4. The steps leading to the values of χ are the same as those in Section 4.2 where we calculated the Bishop parameter per Voigt estimate of effective bulk properties, only now the micromechanical estimates of effective properties are mathematically more involved. Additionally, in order to generate specific theoretical values of the Bishop parameter it now becomes necessary to assume an overall material porosity, ϕ, which conveniently reduced out of the earlier calculations. We assume the overall porosity of 30%, common to all model materials, in order to include a greater range of

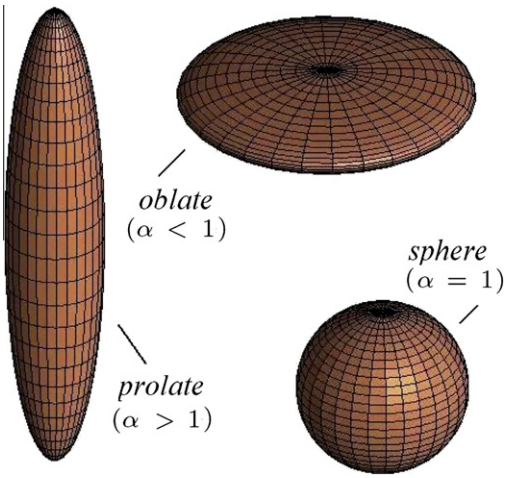

Fig. 3. Idealized spheroidal shapes characterized by an aspect ratio α, used to describe inclusion shapes in multiphase materials. In porous materials, voids in the shape of oblates ($\alpha < 1$, 'flat' sphere) mimic crack-like cavities. Voids or solid inclusions in the shape of prolates ($\alpha > 1$, 'stretched' sphere) mimic needle-like cavities in porous materials or needle-like particles in granular materials respectively. $\alpha = 1$ for a sphere. See Appendix A for further details and practical examples.

K_b/K_s ratios as well as very low ratios of K_b/K_s, as evident from Fig. 4. To provide a common thread, a poisson ratio of $\nu = 0.25$ is assumed common for all solids or grains; for variations up to ±0.1 in Poisson ratio the predictions vary only slightly.

In analyzing the results of Fig. 5, we find that for materials well-described by the Mori–Tanaka micromechanical estimate (and by the Voigt estimate as shown in Section 4.2), the Bishop parameter remarkably reduces to S_w. Note that this is true for an MT material of any porosity and of any aspect ratio of randomly oriented and homogeneously distributed pores of ellipsoidal shape, as shown analytically in Appendix B. As we noted in Section 3.2, this relationship has also been found from the entropy inequality, via the macroscopic volume averaging, and on the basis of mixture theory. It is also the most commonly utilized expression for χ in literature today.

More importantly, it is evident from Fig. 5 that in general $\chi \neq S_w$ and that instead χ takes on a value that depends on the morphological features of the model material at any degree of partial saturation. This helps explain why the Bishop parameter is often reported to depend on material fabric. We should caution against arriving at specific conclusions regarding the ranges and values of χ from Fig. 5. Presently, we only show sample predictions for materials of a single overall porosity and Poisson ratio, 30% and 0.25, respectively. Other combination of assumed material properties can yield different values of χ, as can different assumptions regarding the pore geometries and/or different homogenization schemes. Nevertheless we should add that for a great number of combinations we examined, the Bishop parameter appears to always take on a value above $\chi = S_w$ line. Therefore our formulation tentatively suggests that $\chi = S_w$ line represents the lower bound of possible values of χ.

4.4. Limitations

We should remark that our proposed effective stress expression in Eq. (7), and thus the predictions of the Bishop parameter in Fig. 5, captures the effects of capillary pressure in controlling the elastic volume change of partially saturated materials. The capillary pressure however may also influence other properties such as the shear stiffness (e.g. Fournier et al., 2005) which are not accounted for here. In addition to the capillary pressure, the effects of the surface tension effects and of the disjoining pressure may be influential, particularly at low values of saturation, when the wetting phase is present as a thin surface film (Gray and Schrefler, 2001). These effects are also largely dependant on the geometric description of the porous

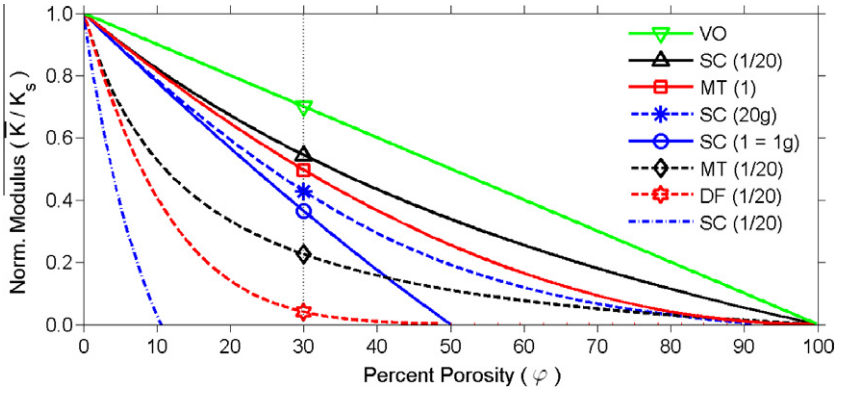

Fig. 4. Effective bulk moduli of an idealized porous material as predicted by following micromechanical schemes: Mori–Tanaka (MT), self-consistent (SC), differential (DF), and Voigt (VO). The number in the legend indicates the aspect ratio α that is common to all randomly oriented spheroidal inclusions, while the letter 'g' next to a number indicates that the solid properties are assigned to the solid inclusions (rather than to the matrix), representing a material composed of grains or crystals. Modulus values are normalized with respect to the elastic properties of a solid, with the Poisson ratio of a solid, ν_s, assumed to be 0.25. For variations up to ±0.1 in Poisson ratio, the predictions vary only slightly. *Note*: Comparably speaking, the spherical ($\alpha = 1$) voids least reduce the overall effective properties of a porous matrix while the crack-like (oblate, $\alpha < 1$) voids have the greatest effect in reducing the effective properties. The predictions for the needle-like (prolate, $\alpha > 1$) inclusions fall somewhere in between the other two (but closer to the predictions based on the spherical voids) and are omitted in order to simplify the figures.

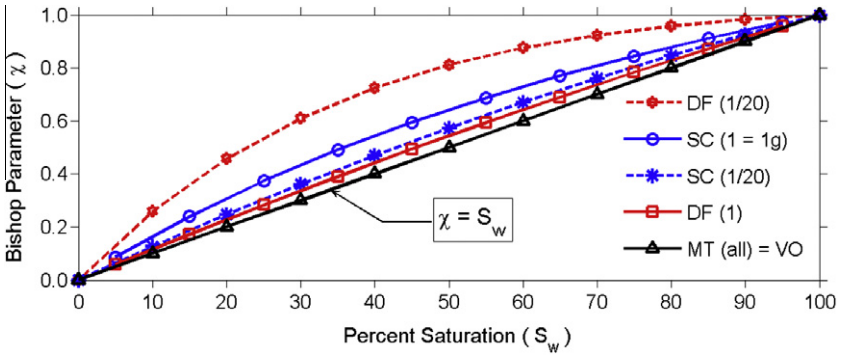

Fig. 5. The Bishop parameter controlling the elastic volume change predicted by our proposed effective stress formulation. Note that materials of any porosity modeled by the Mori–Tanaka (MT) scheme with homogeneously distributed spheroidal pores of any shape, as well as those modeled by the Voigt (VO) scheme, reduce the classic Bishop paramater to $\chi = S_w$, per Eq. (11). Generally, however, the Bishop parameter is not equal to S_w and will instead take on a value that depends on the morphological features of a given porous material. The micromechanical schemes used to estimate the effective bulk properties are shown in Fig. 4. Poisson's ratio of 0.25 and overall drained porosity of 30% is assumed common for all predictions in order to include a greater range as well as very low ratios K_b/K_s, as indicated by an intersecting vertical line in Fig. 4. Note: the Bishop parameter per the self-consistent (SC) scheme with $\alpha = 1/20$ is omitted because the SC scheme predicts the loss of bulk stiffness at ≈11% porosity at this aspect ratio.

material at the micro scale and thus are also not accounted for in our formulation.

We should also remark that the micromechanical schemes employed in this work for the purpose of calculating the Bishop parameter are one-step homogenization estimates. Consequently, the schemes contain restrictions on the relative size of different pores within a material. To explicitly take into account specific pore size distributions or to more accurately account for specific material heterogeneities, more advanced micromechanical techniques may need to be utilized. Nevertheless, as outlined in Appendix A.1 and as evident from Fig. 4, the utilized homogenization estimates show a great diversity of possible effective material properties. As such, using these estimates to quantify the Bishop parameter in Fig. 5 helps answer from a theoretical perspective a question that has proven elusive, namely how sensitive the Bishop parameter is to different material microstructures.

5. Summary

In this work, we present a novel and quantifiable form of effective stress in partially saturated materials. As a backdrop, we provide a historical background and critique of the classic Bishop effective stress in partially saturated materials. Just as in the classic Bishop approach, we find that in the extremes of null and full saturation, our proposed expression seamlessly reduces to the well-known solutions for a dry and a fully saturated porous material, respectively. However, in departure from the previous works, we find that in our proposed expression, the continuity between the dry and the fully saturated extremes is insured via a material parameter, termed the effective Biot coefficient, rather than via a form of the pressure averaging. This finding directly supports the idea that the effective stress in partially saturated materials depends on material fabric, something that has long been observed in literature.

Moreover, we use our findings to address what has been an elusive question thus far: to what extent different materials affect the effective stress expression in partially saturated materials? More specifically, we quantify the value of the Bishop parameter as a function of the (water) saturation for a range of possible material microstructures and morphologies. To this end, we utilize several popular theoretical estimates; to provide a unifying thread, the elastic properties of the solid phase for all estimates are assumed equal. Remarkably, we analytically find that for two specific estimates, the Voigt and the Mori–Tanaka schemes, our formulation reduces to the popular average pressure form with the Bishop parameter equal to the degree of saturation, i.e. $\chi = S_w$. In general, however, we find that $\chi \neq S_w$.

Presently, we analyze material point constitutive behavior at an equilibrium state of partial saturation. For more general problems including the boundary-value problems in which the degree of saturation varies within a cross-section or for inelastic analysis, it would be beneficial to convert the proposed work into its incremental or rate form.

Appendix A. The micromechanical estimates

A.1. Homogenization of an effective solid via micromechanical schemes

We present some solutions for the effective bulk moduli $\overline{K}$ as predicted by the SC, DF, and MT micromechanical schemes in Fig. 4. These solutions are used to quantify the Bishop parameter based on our proposed formulation. For all schemes considered we assume one phase to be a solid material with the Poisson ratio of 0.25; for variations up to ±0.1 in Poisson ratio, the predictions vary only slightly. The other phase is considered degenerate with null bulk and shear stiffness. For MT and DF schemes, the solid material is the matrix with homogeneously dispersed and randomly oriented cavities of spheroidal shape; the aspect ratio α of the spheroidal cavities is indicated by a number in the legend of Fig. 4. Historically, the SC scheme has been used to estimate the properties not only of the porous solids, as were MT and DF schemes, but also of materials composed of individual grains or crystals. In the latter, the roles of the matrix and of the cavities are reversed, i.e. the matrix is assumed

degenerate, while the inclusions are assigned the properties of a solid on physical grounds. We generate these predictions as well and indicate them with letter "g" next to the aspect ratio of the inclusions.

We calculate the effective properties of bodies containing 'randomly oriented spheroidal inclusions' rather than just 'spherical inclusions' because this can be used to model a greater variety of morphological features. These are defined by one additional parameter, the aspect ratio α; the shapes of spheroids with different aspect ratios are shown in inset of Fig. 4. Oblates or "flattened spheres" have proven helpful in representing crack-like cavities (e.g. effective properties of sandstone containing fissures; Prokopiev and Sevostianov, 2007), tending toward so-called penny cracks in the extreme of very low aspect ratios. Prolates or "elongated spheres", with aspect ratios greater than unity, can be used to model needle-like cavities or conversely needle-like solid formations (e.g. properties of a microscopically granular material such as gypsum; Sanahuja et al., 2007).

The effective or homogenized bulk modulus at any given porosity is shown in a normalized form as a fraction of bulk modulus of the solid material. We outline the key observations and trends evident from Fig. 4:

- For all schemes considered, crack-like porous cavities marked by a low aspect ratio tend to cause a steep loss of effective moduli as pore volume is increased. This observation answers why even low porosity materials may have a very low ratio between the (drained) bulk moduli of the porous material and of the solid, and thus be considered incompressible. The trends also help answer why sometimes high porosity materials that contain pores of relatively symmetrical dimensions may in fact prove stiffer than low porosity materials whose pore spaces are a collection of cracks and fissures.
- Given the experimentally measured bounds, the modulus of a solid material K_s and the modulus of the (drained) porous solid K_b (typically measured using (un)jacketed compression tests), a simple linear or first-order estimate of the effective properties is a good approximation provided the pore volume is not composed of crack-like cavities.
- The effective modulus reduces to zero at the extreme of 100% porosity for the MT and the DF schemes. The SC scheme however, predicts a loss of effective stiffness at finite porosity values. Moreover, as pointed out (Sanahuja et al., 2007) and confirmed here, we find that while spherical particles lose volumetric (and shear) stiffness at 50% porosity, a fact often cited as a hallmark of a granular medium, needle-like (prolate) grains are able to maintain stiffness at much higher porosities as predicted by the SC scheme and needle-like granular formations tend to be volumetrically stiffer than a collection of spherical grain.
- The SC scheme does not yield the same properties for granular/crystalline and swiss-cheese type porous material of equal porosity, an observation seldom indicated in literature. It only does so when the inclusions are of spherical shape, which is denoted by $SC(1 = 1g)$ in the legend of Fig. 4.

A.2. Mori–Tanaka, self-consistent, and differential schemes

The expressions for the most commonly encountered micromechanical schemes are in Eqs. (A.1)–(A.3) in their most general form. Tensorial quantities are shown in bold face letters, superscripts i, m indicate the inclusion and matrix phases, respectively, $\sum$ indicates summation over all N individual inclusions, $\overline{\boldsymbol{C}}$ indicates the homogenized or effective property of e.g. material stiffness tensor $\boldsymbol{C}$, $\boldsymbol{I}$ is a symmetric 4th order unit tensor and $\boldsymbol{S}$ is the Eshelby tensor, which depends on inclusion orientation but not on inclusion size. $\boldsymbol{T}$ is often referred to as the strain concentration tensor, due to the fact that physically it describes strain inside an inclusion with respect to the surrounding matrix resulting from an applied far-field loading.

Self-consistent (SC) scheme (Hill, 1965; Budiansky, 1965):

$$\overline{\boldsymbol{C}}_{sc} = \boldsymbol{C}^m + \sum_{r=1}^{N} \varphi_r^i (\boldsymbol{C}_r^i - \boldsymbol{C}^m)\overline{\boldsymbol{T}}_r \tag{A.1}$$

where

$$\overline{\boldsymbol{T}}_r = [\boldsymbol{I} + \overline{\boldsymbol{S}}_r \overline{\boldsymbol{C}}_{sc}^{-1}(\boldsymbol{C}_r^i - \overline{\boldsymbol{C}}_{sc})]^{-1}$$

Mori–Tanaka (MT) scheme (Mori and Tanaka, 1973; Benveniste, 1987):

$$\overline{\boldsymbol{C}}_{mt} = \boldsymbol{C}^m + \sum_{r=1}^{N} \varphi_r^i (\boldsymbol{C}_r^i - \boldsymbol{C}^m)\boldsymbol{T}_r \left[(1-\varphi)\boldsymbol{I} + \sum_{q=1}^{N} \varphi_q^i \boldsymbol{T}_q \right]^{-1} \tag{A.2}$$

where

$$\boldsymbol{T}_{r;q} = [\boldsymbol{I} + \boldsymbol{S}_{r;q}(\boldsymbol{C}^m)^{-1}(\boldsymbol{C}_{r;q}^i - \boldsymbol{C}^m)]^{-1}$$

Differential (DF) scheme (Hashin, 1988; Berryman et al., 2002; Giordano, 2003):

$$\frac{d\overline{\boldsymbol{C}}_{df}}{d\varphi} = \frac{1}{1-\varphi}(\boldsymbol{C}^i - \overline{\boldsymbol{C}}_{df}) \sum_{r=1}^{N} \overline{\boldsymbol{T}}_r; \quad \overline{\boldsymbol{C}}_{df}(0) = \boldsymbol{C}^m \tag{A.3}$$

where

$$\overline{\boldsymbol{T}}_r = [\boldsymbol{I} + \overline{\boldsymbol{S}}_r(\overline{\boldsymbol{C}}_{df})^{-1}(\boldsymbol{C}_r^i - \overline{\boldsymbol{C}}_{df})]^{-1}$$

It should be noted that the aforementioned schemes cannot take into account the inclusions that are non-homogeneously distributed. Zheng and Du (2001) provide a good historical overview on the topic and offer ways to overcome this limitation.

A.3. Numerical evaluation of the schemes: the spheroid inclusion shapes

Here we restrict ourselves to evaluating the properties of an isotropic solid containing randomly oriented spheroidal inclusions. The random orientation of the inclusions insures that overall properties of the *effective solid* are isotropic even if the individual inclusions are not isotropic. A spheroidal shape is used to describe non-spherical inclusions with minimum number of parameters, as shown in the inset of Fig. 4. We note that when the inclusions reach a high enough aspect ratios, the effective properties may

no longer depend on porosity but rather on a variable such as a crack density parameter. At present, we consider aspect ratios, α, up to 1/20 and 20 for oblates and prolates respectively not with the intention of making specific predictions but rather of determining patterns of behavior of effective properties as e.g. pore shapes tend toward cracks.

We next briefly summarize a numerical method used to generate micromechanical estimates based on Eq. (A.1)–(A.3). An integral expression replaces the summation given an orientation distribution $f(\Phi, \Theta)$ of spheroidal inclusions, per recipe shown in Eq. (A.4), where Φ and Θ are Euler angles that define orientation direction as points on a unit sphere:

$$\sum_{r=1}^{N} \diamondsuit_r \Rightarrow \frac{1}{4\pi}\int_0^{2\pi}\int_0^{\pi} f(\Phi,\Theta)\diamondsuit(\Phi,\Theta) sin\Theta d\Phi d\Theta \tag{A.4}$$

Random orientation means that each inclusion has an equal probability of being oriented in any arbitrary direction, resulting in a probability density function $f(\Phi,\Theta) = 1$. The components of the Eshelby tensor $\boldsymbol{S}$ can be found in Mura (1987, p. 84) for a fixed and convenient reference frame. The Eshelby tensor for any other arbitrary inclusion orientation is found by applying standard transformation rules for a 4th order tensor using Euler angles Φ,Θ. As a result of the ensuing complexity of the Eshelby tensor $\boldsymbol{S}$, and thus of the strain concentration tensor $\boldsymbol{T}$, the integration is performed numerically using Gauss points; 15 Gauss points on the interval of $0-\pi$ for each Euler angle (for a total of 450 Gauss points) provide a sufficient degree of accuracy while minimizing computational time. Following the integration, all schemes are reduced to two scalar equations, by decomposing the isotropic tensorial expressions into its spherical and deviatoric components.

The MT scheme is explicit and thus the predictions of the bulk modulus at any given porosity can be evaluated directly. The SC scheme is implicit, and upon scalar simplification, yields two coupled non-linear equations involving bulk and shear moduli. The SC scheme was solved iteratively via an implicit Newton–Raphson solver, with the Jacobian evaluated numerically at each step. For the differential scheme, an explicit fourth order Runga–Kutta method was used to approximate a solution to two coupled ordinary differential equations. As a check, the numerical solutions were compared to the analytical ones available in the case of spherical inclusions. In all cases considered, the accuracy to within 1/100th of a percent was obtained.

Appendix B. Bishop parameter χ for a Mori–Tanaka type material: the analytical solution

From Eq. (A.2), a general Mori–Tanaka estimate of the homogenized material tensor $\overline{\boldsymbol{C}}_{mt}$ at a porosity φ reads:

$$\overline{\boldsymbol{C}}_{mt} = \boldsymbol{C}^m + \sum_{r=1}^{N} \varphi_r^i (\boldsymbol{C}_r^i - \boldsymbol{C}^m)\boldsymbol{T}_r \left[(1-\varphi)\boldsymbol{I} + \sum_{q=1}^{N}\varphi_q^i \boldsymbol{T}_q\right]^{-1} \tag{B.1}$$

Noting that the inclusion material tensor $\boldsymbol{C}^i$ is null and that the solid (matrix) material tensor $\boldsymbol{C}^m$ is finite and isotropic we deduce via Eq. (A.4) that:

$$\sum_{r=1}^{N} \varphi_r^i \left(\boldsymbol{C}_r^i - \boldsymbol{C}^m\right)\boldsymbol{T}_r \Rightarrow \varphi \boldsymbol{C}^m \left[\underbrace{\frac{-1}{4\pi}\int_0^{2\pi}\int_0^{\pi} f(\Phi,\Theta)\boldsymbol{T}(\Phi,\Theta) sin\Theta d\Phi d\Theta}_{\boldsymbol{\Omega}}\right] \tag{B.2}$$

Where the porous inclusions of similar shape are randomly oriented in space, the orientation probability density $f(\Phi,\Theta) = 1$ and the tensorial quantity $\boldsymbol{\Omega}$ is isotropic. Writing the spherical part of Eq. (B.1) leads to:

$$\begin{aligned}\overline{K}_{mt} &= K^m - \varphi K^m \kappa [1 - \varphi + \varphi\kappa]^{-1} \\ &= K^m \frac{1-\varphi}{1-\varphi(1-\kappa)}\end{aligned} \tag{B.3}$$

where κ is a scalar multiplier of the spherical part of isotropic $\boldsymbol{\Omega}$; the exact value of κ is of little importance since it will eventually reduce out of Eq. (B.4). We now return to Eq. (11) and seek to evaluate the Bishop parameter χ under the assumption that the elastic properties of the *effective solid* are well-represented by the Mori–Tanaka micromechanical scheme:

$$\chi^{mt} = \frac{1 - (K_b^{mt}/K_s)(K_s/\overline{K}_{mt})}{1 - K_b^{mt}/K_s}; \tag{B.4}$$

where

$$K_s = K^m$$

$$\overline{K} = \overline{K}_{mt}(\varphi) = K_s \frac{1-\varphi}{1-\varphi(1-\kappa)}$$

$$K_b^{mt} = \overline{K}_{mt}(\varphi = \phi_o) = K_s \frac{1-\phi_o}{1-\phi_o(1-\kappa)}$$

where we assign the solid properties to the matrix material and where at porosity of $\varphi = \phi_o$, $\overline{K}_{mt}$ reduces to the (drained) bulk modulus K_b^{mt}. Let us first resolve the divisor of Eq. (B.4):

$$1 - K_b^{mt}/K_s = 1 - \left(\frac{1-\phi_o}{1-\phi_o(1-\kappa)}\right) = \frac{\phi_o\kappa}{1-\phi_o(1-\kappa)} \tag{B.5}$$

followed by the dividend, via Eq. (4):

$$\begin{aligned}1 - \frac{K_b^{mt}}{K_s}\frac{K_s}{\overline{K}_{mt}} &= 1 - \left(\frac{1-\phi_o}{1-\phi_o(1-\kappa)}\right)\left(\frac{1-\varphi}{1-\varphi(1-\kappa)}\right)^{-1} \\ &\text{where} \quad \varphi = \varphi(S_w) = \frac{(1-S_w)\phi_o}{1-S_w\phi_o} \\ &= 1 - \left(\frac{1-\phi_o}{1-\phi_o(1-\kappa)}\right)\left(\frac{1-\phi_o(1-\kappa(1-S_w))}{1-\phi_o}\right) \\ &= \frac{S_w\phi_o\kappa}{1-\phi_o(1-\kappa)}\end{aligned} \tag{B.6}$$

Ultimately, the Bishop parameter strikingly simplifies to:

$$\begin{aligned}\chi^{mt} &= \frac{1 - (K_b^{mt}/K_s)(K_s/\overline{K}_{mt})}{1 - K_b^{mt}/K_s} \\ &= \frac{S_w\phi_o\kappa/(1-\phi_o(1-\kappa))}{\phi_o\kappa/(1-\phi_o(1-\kappa))} \\ \chi^{mt} &= S_w\end{aligned} \tag{B.7}$$

We have thus shown that our proposed formulation, under the assumption that the properties of a given porous material may be described by the Mori–Tanaka micromechanical scheme, reduces to the popular form of Bishop's effective stress, namely $\chi(S_w) = S_w$.

References

Aitchison, G.D., Bishop, A.W., 1960. Discussion in Proc. Conf. Pore Pressure and Suction in Soils. Butterworth, London. p. 150.

Alonso, E.E., Delage, P. (Eds.), 1996. Unsaturated Soils. Balkema, Roterdam, Netherlands.

Alonso, E.E., Gens, A., Josa, A., 1990. A constitutive model for partially saturated soils. Géotechnique 40 (3), 405430.

Benveniste, Y., 1987. A new approach to the application of Mori–Tanaka's theory in composite materials. Mechanics of Materials 6, 147–157.

Berryman, J.G., Pride, S.R., Wang, H.F., 2002. A differential scheme for elastic properties of rocks with dry or saturated cracks. Geophysical Journal International 151 (2), 597–611.

Bishop, A.W., 1955. Lecture delivered in Oslo, Norway, entitled 'The principle of effective stress' (Printed in Teknisk Ukeblad 39 (1959) 859–863).

Bishop, A.W., Blight, G.E., 1963. Some aspects of effective stress in saturated and partly saturated soils. Géotechnique 13 (3), 177–197.

Bishop, A.W., Eldin, A., 1950. Undrained triaxial tests on saturated sands and their significance in the general theory of shear strength. Géotechnique 2 (1), 13–32.

Budiansky, B., 1965. On elastic moduli of some heterogeneous materials. Journal of the Mechanics and Physics of Solids 13 (4), 223–227.

Chateau, X., Dormieux, L., 2002. Micromechanics of saturated and unsaturated porous media. International Journal for Numerical and Analytical Methods in Geomechanics 26 (8), 831–844.

Coleman, J.D., 1962. Stress-strain relations for partially saturated soils. Géotechnique 12 (4), 348–350.

Coussy, O., 2008. Revisiting the constitutive equations of unsaturated porous solids with a Lagrangian saturation concept. International Journal of Numerical and Analytical Methods in Geomechanics 31 (15), 1675–1694.

de Boer, R., 1992. Development of porous media theories – a brief historical review. Transport in Porous Media 9, 155–164.

Dormieux, L., Kondo, D., Ulm, F.-J., 2006. Microporomechanics. John Wiley and Sons.

Fournier, Z., Geromichalos, D., Herminghaus, S., Kohonen, M.M., Mugele, F., Scheel, M., Schulz, M., Schulz, B., Schier, C., Seemann, R., Skudelny, A., 2005. Mechanical properties of wet granular materials. Journal of Physics: Condensed Matter 17 (9), S477.

Fredlund, D.G., Morgenstern, N.R., 1977. Stress state variables for unsaturated soils. ABB Review 103 (5), 447–466.

Geertsma, J., 1957. The effect of fluid pressure decline on volumetric changes of porous rocks. Transactions of AIME 210, 331.

Gens, A., Sánchez, M., Sheng, D., 2007. On constitutive modelling of unsaturated soils. Acta Geotechnica 1 (3), 137–147.

Giordano, S., 2003. Differential schemes for the elastic characterisation of dispersions of randomly oriented ellipsoids. European Journal of Mechanics A/Solids 22 (6), 885–902.

Gray, W.G., Schrefler, B.A., 2001. Thermodynamic approach to effective stress in partially saturated porous media. European Journal of Mechanics A/Solids 20 (4), 521–538.

Grueschow, E., Rudnicki, J.W., 2005. Elliptic yield cap constitutive modeling for high porosity sandstone. International Journal of Solids and Structures 42 (16-17), 4574–4587.

Gudehus, G., 1995. A comprehensive concept for non-saturated granular bodies. In: Proc. of the 1st International Conference on Unsaturated Soils, Paris, France.

Hashin, Z., 1988. The differential scheme and its application to cracked materials. Journal of the Mechanics and Physics of Solids 36 (6), 719–734.

Hassanizadeh, S.M., Gray, W.G., 1980. General conservation equations for multiphase systems: III Constitutive theory for porous media flow. Advances in Water Resources 3 (1), 25–40.

Hill, R., 1965. A self-consistent mechanics of composite materials. Journal of the Mechanics and Physics of Solids 13 (4), 213–222.

Hutter, K., Laloui, L., Vulliet, L., 1999. Thermodynamically based mixture models of saturated and unsaturated soils. Mechanics of Cohesive-Frictional Materials 4 (4), 295–338.

Jennings, J.E., Burland, J.B., 1962. Limitations to the use of effective stresses in partly saturated soils. Géotechnique 12 (2), 125–144.

Khalili, N., Geiser, F., Blight, G.E., 2004. Effective stress in unsaturated soils: review with new evidence. International Journal of Geomechanics 4 (2), 115–126.

Khalili, N., Khabbaz, M.H., 1998. A unique relationship for χ for the determination of shear strength of unsaturated soils. Géotechnique 48 (5), 681–688.

Laughton, A.S., 1955. The Compaction of Ocean Sediments. Ph.D. Thesis, University of Cambridge.

Lewis, R.W., Schrefler, B.A., 1987. The Finite Element Method in the Deformation and Consolidation of Porous Media. John Wiley and Sons, Chichester.

Mori, T., Tanaka, K., 1973. Average stress in matrix and average elastic energy of materials with misfitting inclusions. Acta Metallurgica 21, 571–574.

Mura, T., 1987. Micromechanics of Defects in Solids, second ed. Kluwer Academic, Dordrecht.

Nur, A., Byerlee, J.D., 1971. An exact effective stress law for elastic deformation of rock with fluids. Journal of Geophysical Research 76, 6414–6419.

Prokopiev, O., Sevostianov, I., 2007. Modeling of porous rock: digitization and finite elements versus approximate schemes accounting for pore shapes. International Journal of Fracture 143 (4), 369–375.

Sanahuja, J., Dormieux, L., Chanvillard, G., 2007. Modelling elasticity of a hydrating cement paste. Cement and Concrete Research 37, 1427–1439.

Santagiuliana, R., Schrefler, B.A., 2006. Enhancing the Bolzon–Schrefler–Zienkiewicz constitutive model for partially saturated soil. Transport in Porous Media 65 (1), 1–30.

Schofield, A., Wroth, P., 1968. Critical State Soil Mechanics. McGraw-Hill, New York, NY.

Sheng, D., Gens, A., Fredlund, D.G., Sloan, S.W., 2008. Unsaturated soils: from constitutive modelling to numerical algorithms. Computers and Geotechnics 35 (6), 810–824. doi:10.1016/j.compgeo.2008.08.011.

Sheng, D., Sloan, S.W., Gens, A., 2004. A constitutive model for unsaturated soils: thermomechanical and computational aspects. Computational Mechanics 33 (6), 453–465. doi:10.1007/s00466-003-0545-x.

Skempton, A.W., 1961. Effective stress in soils, concrete and rock. concrete. Proceedings of Conference on Pore Pressure and Suction in Soils. Butterworth, London, England. pp. 4–16.

Vlahinić, I., Jennings, H.M., Thomas, J.J., 2009. A constitutive model for drying of a partially saturated porous material. Mechanics of Materials 41 (3), 319–328.

Walsh, J.B., Brace, W.F., England, A.W., 1965. Effect of porosity on compressibility of glass. Journal of American Ceramics Society 48 (12), 605–608.

Wheeler, S.J., Sivakumar, V., 1995. An elasto-plastic critical state framework for unsaturated soil. Géotechnique 45 (1), 35–53.

Zheng, Q.-S., Du, D.-X., 2001. An explicit and universally applicable estimate for the effective properties of multiphase composites which accounts for inclusion distribution. Journal of the Mechanics and Physics of Solids 49 (11), 2765–2788.

Zienkiewicz, O., Chan, A., Pastor, M., Schrefler, B., Shiomi, T., 1999. Computational Geomechanics. John Wiley and Sons, Chichester.